Finite Element Analysis of Welding Distortion in a Large Thin-plate Panel Structure[†]

Dean Deng *, Ninshu Ma **, and Hidekazu Murakawa ***

Abstract

Welding distortion not only negatively affects the dimensional accuracy but also significantly degrades the quality and performance. Although many researchers and engineers have made great efforts to control and reduce welding deformation, it is still a difficult engineering problem. In the current study, welding distortion in a large thin-plate panel structure was predicted by means of elastic FEM based on inherent strain theory and interface element formulation. The welding distortions in the thin-plate model computed by large deformation theory and by small deformation theory were compared. In addition, the influences of welding procedure and assembly sequence on the final distortion were examined numerically.

1. Introduction

Fusion welding process is widely used in shipbuilding and automobile industries to join thin plate panel structures. In recent years, high tensile strength steel thin plate has been used to replace low carbon steel for reducing weight. However, buckling propensity induced by the welding process will increase when the thickness of the plate decreases. Buckling distortion often not only results in loss of structural integrity and dimensional accuracy, but also increases fabrication cost due to correction work. For thin-plate panel structures, if welding distortion and buckling propensity can be quantitatively predicted beforehand, the predictions will be useful and helpful to improve manufacturing accuracy.

In the past decades, a number of finite element models and experimental methods have been proposed to study welding distortion in thin-plate structures. Watanabe and Satoh [1] investigated welding deformation in thin plates due to bead-on welding. Nomoto and his co-workers [2, 3] studied the parameters controlling buckling distortion using both experimental and numerical methods. Tasi et al. [4] studied the bifurcation phenomenon in thin plate joint using thermo-elastic-plastic, large deformation analysis and experiments. Michaleries et al. [5] compared the buckling propensity for SAW, GMAW and FSW using butt-joints. Huang and Dong [6, 7] have developed fabrication and engineering technologies for lightweight ship structures. In their researches, some significant progresses have been achieved to control welding distortion especially buckling distortion. Deo and Michaleris [8] studied how to mitigate buckling distortion induced by welding using transient thermal tensioning.

Although the above researchers had made large contributions to the control of buckling distortion induced by welding, their research objects almost were limited to the laboratory specimens. Welding distortion and buckling propensity in large structures requires further research. In addition, investigation is needed to incorporate tack welding and welding sequence in computational approaches [9].

In this study, welding distortion in a large thin-plate panel structure was predicted by means of elastic FEM based on inherent strain theory and interface element formulation. The welding distortions in the thin-plate model computed by large deformation theory and small deformation theory were compared. In addition, the influences of welding procedure and assembly sequence on the final distortion were examined numerically.

2. Concepts of inherent strain and inherent deformation

During welding process, the mechanical behavior is very complicated. Generally, the total strain ε can be

decomposed into the elastic strain ε^e, plastic strain ε^p, thermal strain ε^T, creep strain ε^c and that produced through phase transformation ε^{tr}.

$$\varepsilon = \varepsilon^e + \varepsilon^p + \varepsilon^T + \varepsilon^c + \varepsilon^{tr} \tag{1}$$

Noting that the deformation and the stress are produced by the total strain ε and the elastic strain ε^e, Eq. (1) can be rearranged to,

$$\varepsilon - \varepsilon^e = \varepsilon^p + \varepsilon^T + \varepsilon^c + \varepsilon^{tr} = \varepsilon^* \tag{2}$$

This equation means that the distortion and the residual stress are produced by the inherent strain ε^* which consists of plastic, thermal, creep strains and that caused by the phase transformation.

Welding deformations in a thin plate such as the transverse shrinkage, the longitudinal shrinkage and the angular distortion are mostly produced by the longitudinal and the transverse inherent strains ε_x^* and ε_y^*. By integrating the inherent strain over the cross-section normal to the welding line and taking the average value through the thickness h, the inherent deformations are obtained [10].

Longitudinal shrinkage:

$$\delta_L^* = \tfrac{1}{h}\iint \varepsilon_x^* \, dydz \tag{3}$$

Transverse shrinkage:

$$\delta_T^* = \tfrac{1}{h}\iint \varepsilon_y^* \, dydz \tag{4}$$

Longitudinal bending:

$$\theta_L^* = \tfrac{12}{h^3}\iint (z - h/2)\varepsilon_x^* \, dydz \tag{5}$$

Transverse bending (Angular distortion):

$$\theta_T^* = \tfrac{12}{h^3}\iint (z - h/2)\varepsilon_y^* \, dydz \tag{6}$$

Further, longitudinal shrinkage is often represented by Tendon Force [11, 12] which can be calculated by the following equation.

$$F_T = E\iint \varepsilon_x^* \, dydz \tag{7}$$

where, E is Young's modulus of base metal or weld metal at room temperature.

The inherent deformations can be obtained through thermal elastic plastic finite element analysis and experimental method [13]. When the inherent deformations of each joint in a welded structure are known, the overall welding distortion can be calculated using the elastic FEM based on inherent strain theory.
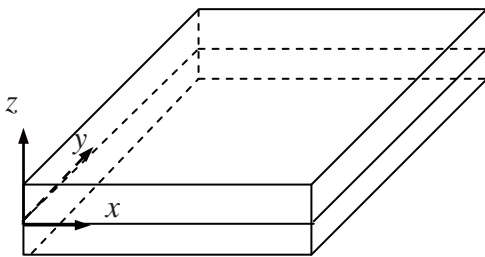

Fig. 1 Rectangular plate and its coordinate system

3. Elastic FEM based on Inherent Strain and Interface Element
3.1 Inherent strain method

In the developed elastic FEM, four-node shell elements (ordinary elements) are used to model every part in a welded structure. In the ordinary elements, the Mindlin plate theory is employed. Meanwhile, the geometrical nonlinear effect is also considered in the shell element. **Fig. 1** shows a thin rectangular plate and its coordinate system. By considering transverse shear strain effects, the total strain of each component can be expressed using the following equations.

$$\varepsilon_x = \varepsilon_x^i + \varepsilon_x^b = \left[\frac{\partial u}{\partial x} + \frac{1}{2}\left(\frac{\partial w}{\partial x}\right)^2 \right] + \left[-z\frac{\partial^2 w}{\partial x^2} + z\frac{\partial \theta_y}{\partial x} \right] \tag{8}$$

$$\varepsilon_y = \varepsilon_y^i + \varepsilon_y^b = \left[\frac{\partial v}{\partial y} + \frac{1}{2}\left(\frac{\partial w}{\partial y}\right)^2 \right] + \left[-z\frac{\partial^2 w}{\partial y^2} - z\frac{\partial \theta_x}{\partial y} \right] \tag{9}$$

$$\gamma_{xy} = \gamma_{xy}^i + \gamma_{xy}^b = \left[\frac{\partial u}{\partial y} + \frac{\partial v}{\partial x} + \left(\frac{\partial w}{\partial x}\right)\left(\frac{\partial w}{\partial y}\right) \right] + \left[-2z\frac{\partial^2 w}{\partial x\partial y} + z\frac{\partial \theta_y}{\partial y} - z\frac{\partial \theta_x}{\partial x} \right] \tag{10}$$

$$\gamma_{xz} = \theta_y + \frac{\partial w}{\partial x} \tag{11}$$

$$\gamma_{yz} = -\theta_x + \frac{\partial w}{\partial y} \tag{12}$$

Where, u and v, are in-plane displacements at the mid-plane; w is out-of-plane displacement; θ_x and θ_y are rotations around x-axis and y-axis; ε_x, ε_y, are normal strains in x-direction and y-direction; $\gamma_{xy,}$ is the shear strain in the x-y plane; ε_x^i, ε_y^i and γ_{xy}^i are in-plane strains; ε_x^b, ε_y^b and γ_{xy}^b are bending strains; and γ_{xz} and $\gamma_{y,z,}$ are transverse shear strains.

The curvature κ_x in a plane parallel to the x-z plane, the curvature κ_y in a plane parallel to the y-z plane and the twisting curvature κ_{xy}, representing the warping of the x-y plane can be defined as follows [14].

$$\kappa_x = -\frac{\partial^2 w}{\partial x^2} \tag{13}$$

$$\kappa_y = -\frac{\partial^2 w}{\partial y^2} \tag{14}$$

$$\kappa_{xy} = -\frac{\partial^2 w}{\partial x\partial y} \tag{15}$$

In the present elastic FEM, method four types of inherent deformations, namely longitudinal shrinkage, transverse shrinkage, longitudinal bending and angular distortion can be introduced into the elastic FEM. When a welding line is arranged parallel to the x-axis, longitudinal shrinkage (or Tendon force) can be transformed into an in-plane strain component $\bar{\varepsilon}_x^*$ in the longitudinal direction, while transverse shrinkage can be changed into in-plane strain component $\bar{\varepsilon}_y^*$ in the transverse direction. In the similar way, longitudinal bending and angular distortion can be converted into

curvatures $\bar{\kappa}_x^*$ and $\bar{\kappa}_y^*$, respectively. In many cases, because the longitudinal bending is very small it is often neglected. **Fig. 2** schematically shows an example of how to introduce inherent strains into the area around the welding line in a fillet joint. It is assumed that each inherent strain component along the welding line has uniform distribution.

3.2 Features and functions of interface element

When a fusion welding method is used to assemble a large structure, the entire assembly process can be regarded as sequentially positioning new parts onto a reference part and joining them. Physically, the contact relationships between two parts are free before positioning. When the two parts are positioned, the distance between them is pulled to a level within a tolerable limit. In addition, the gap and the misalignment due to the initial geometrical error or induced by

sequential welding can also be corrected in the course of positioning process. Hence, a relatively tight contact relationship between them is formed after positioning. After welding, a very strong bonding between the parts is generated. In order to model the real assembly process, the change of physical status must be carefully taken into account. In particular, the positioning process must be modeled cautiously with considering contact, slide and gap between parts. For this purpose, the interface element [15, 16] is introduced in the elastic FEM. Furthermore, the interface element can describe the change of stiffness during the assembly process. Hence, besides modeling the generation of a gap and its correction, the interface element can also simulate how welding sequence affects the final distortion.

Interface element is nothing but a nonlinear spring with special properties and inserted between members as shown in **Fig. 3**. The relative displacements or the discontinuities of the deformation across the interface
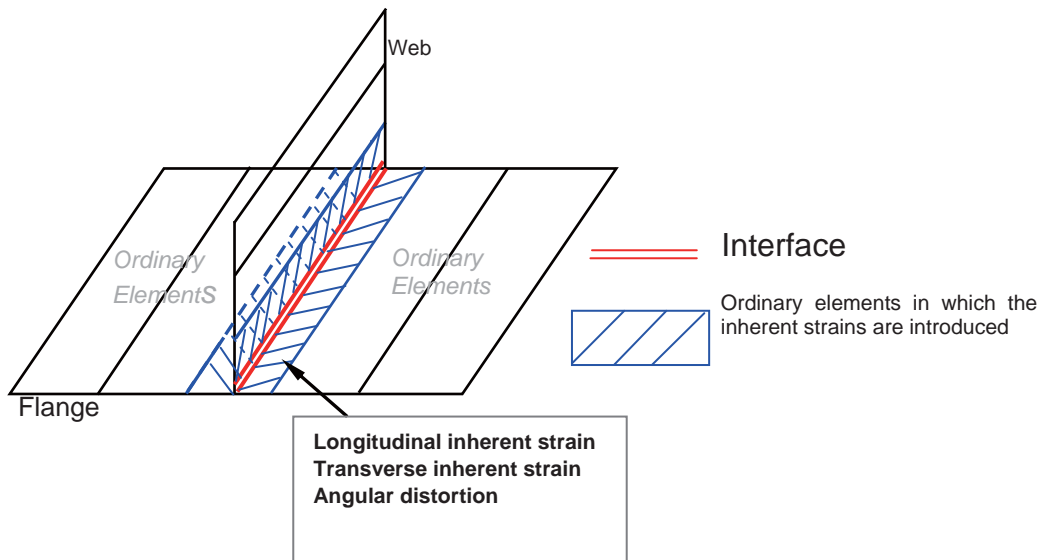

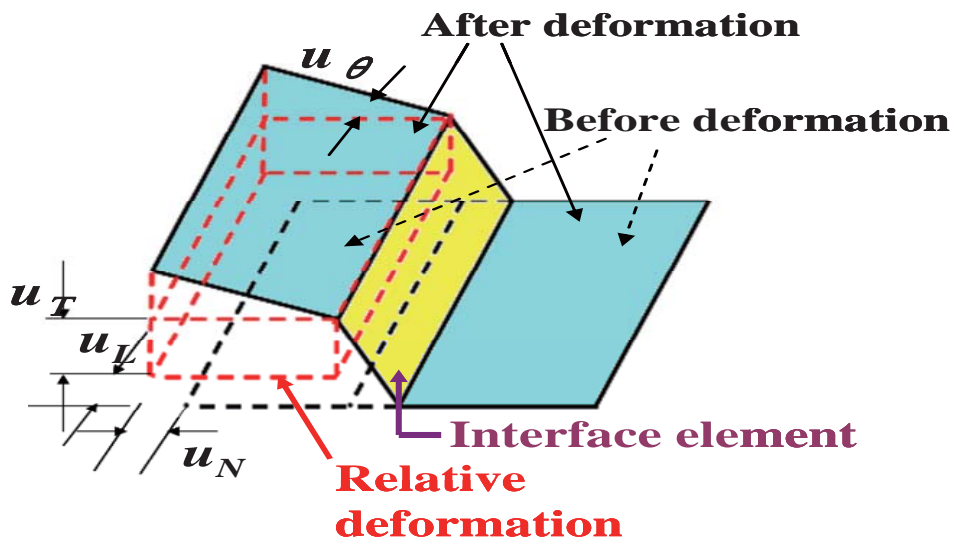**Fig.2** Elements with inherent deformations and agreement of interface elements in a T-joint

Fig. 3 Definition of displacement in interface element

element in the welding direction, in the normal direction and in the transverse direction are denoted as u_L, u_N, u_T. The rotation around the welding direction is denoted by u_θ. The forces or a moment associated with these displacements are denoted by f_L, f_N, f_T and f_θ. The relations between the displacements and the forces are illustrated in **Fig. 4.** The mechanical properties of the nonlinear spring are controlled by the stiffness K, the maximum force f_{max} and the gap u_G. When the members are free, $K = 0$. In the fitting stage, the value of stiffness K for each direction is set to an appropriate value according to the type of tack welding or the fixture. The gap in the fitting stage can be controlled by the values of K and f_{max}. As shown in **Fig. 4**, K is the slope of the straight line which describes the force-displacement relationship of the interface element, and it is determined by parameter f_{max} and scale parameter r_0. In the interface elements, scale parameter r_0 mainly dominates the positioning accuracy. Hence, during positioning process, through adjusting f_{max} and r_0 an appropriate value of K can be obtained. When the joint is fully connected after welding, the stiffness is set to be a large enough value. **Table 1** shows the recommended values of the parameters used in interface elements at different stages.

Table 1 Parameters of interface element used in different stage

State	f_{max} (N/mm)	r_0 (mm)	K
Free	10^{-5}	10^3	≈ 0
Positioning	$10^{0\sim2}$	$10^{-1\sim-2}$	relatively large
Welding	10^{10}	10^3	very large
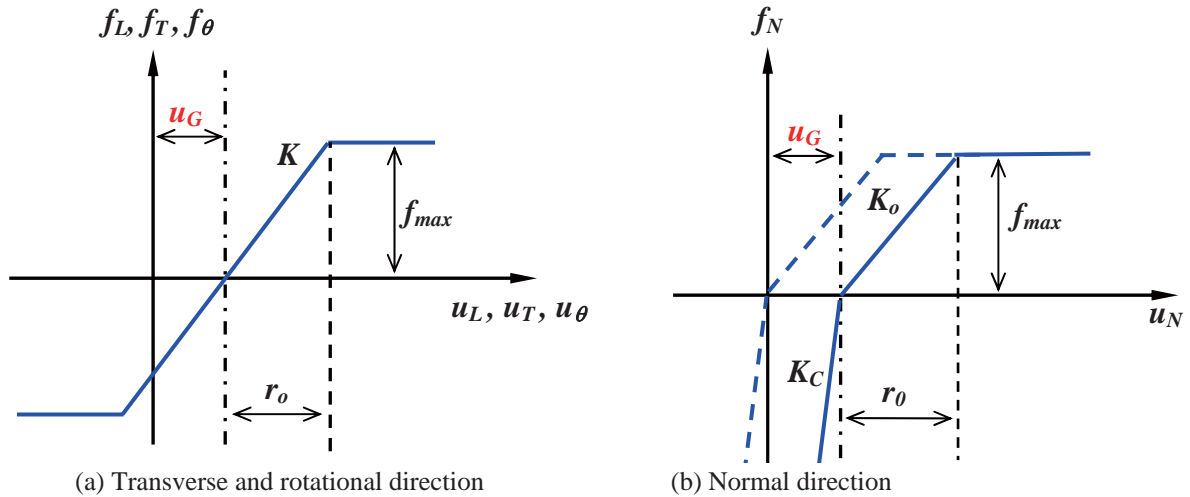
3.3 Computational approach

For a large welded structure, after obtaining the inherent deformations of each joint and determining the parameters of interface elements during the assembly process, we can use the proposed elastic FEM to estimate the overall welding distortion. The computational approach based on inherent strain theory and interface element formulation is schematically shown in **Fig. 5.**

4. Predicting welding distortion in a thin-plate panel structure

4.1 Thin-plate panel structure

To investigate the features of welding deformation using inherent strain and interface element, a finite element model with large dimensions shown in **Fig. 6** was developed in the current work. The material of this thin-plate panel structure is assumed to be Thermo-mechanical control process steel with 570MPa tensile strength. The length of the skin plate is 12000 mm, the width is 4000 mm, and the thickness is 5 mm. There are three longitudinal stiffeners with 1000 mm span and four transverse stiffeners with 3000 mm span in the model. The height of transverse stiffeners is 300 mm, and that of longitudinal stiffeners is 125 mm.

From **Fig. 6**, we can know that there are two typical joints. One is the fillet joint between the longitudinal (or transverse) stiffeners and the skin plate, and the other is the cross-shaped joint between longitudinal stiffeners and transverse stiffeners. Here, it should be stressed that because the thickness of both the longitudinal stiffeners and the transverse stiffeners is 9 mm, even though the height of the longitudinal stiffeners is smaller than that of the transverse stiffeners we can just use one typical joint to represent the two fillet joints between the stiffeners and the skin plate. All the welding lines are denoted by solid lines. There are two weld passes in each fillet joint and four passes in each cross-shaped joint. The interface elements are arranged along each welding line between the two parts to be welded. Before welding, it was assumed that there were no geometrical errors in all parts. In other words, there were no initial gaps in the finite

(a) Transverse and rotational direction   (b) Normal direction

Fig. 4 Mechanical properties of interface element

element model.

Because the thickness of skin plate is only 5 mm, it can be inferred that buckling distortion will potentially occur after welding. To prevent too large distortion, a relatively strong restraint conditions were applied to the finite element model. In **Fig. 6**, the restraint conditions are denoted by the black arrows.

4.2 Welding conditions and Inherent deformations

In this study, to clarify the influence of welding procedure on the final distortion, it was assumed that the fillet joints were performed by two methods. One is double-sided welding, and the other is single-sided welding. CO_2 gas arc metal welding was assumed to perform the welding, and the welding parameters for each side are given in **Table 2**. Single-sided welding was assumed to perform the cross-shaped joints, and the welding conditions for each weld pass are also shown in **Table 2.** The efficiency was assumed to be 0.85 [17].

Table 2 Welding conditions used in fillet joint and cross-shaped joint

Parameters	Current (A)	Voltage (V)	Speed (mm/min)
Fillet Joint	250	25	600
Cross-shaped Joint	225	20	600

Using thermo-elastic-plastic FEM, the inherent deformations of each joint can be estimated. The finite element models of two typical joints are schematically shown in **Fig. 5**. The detailed computational approach can be found in Ref. [13, 18], so we only report the simulation results in the current paper. The inherent deformations of the fillet joint and the cross-shaped joint are shown in **Table 3**. Three inherent deformation components of the fillet joint are used to predict the total welding distortion in the whole structure, and the longitudinal bending was neglected because of
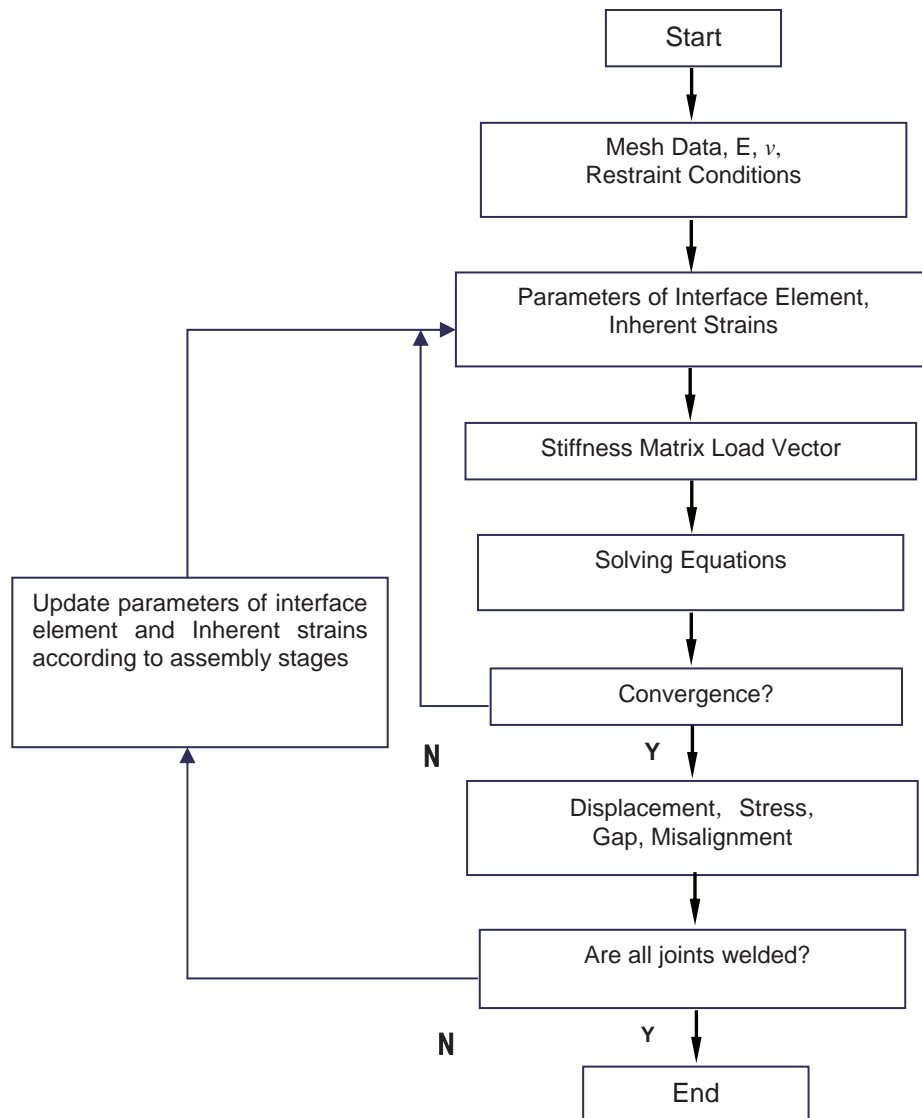
Start

Mesh Data, E, v, Restraint Conditions

Parameters of Interface Element, Inherent Strains

Stiffness Matrix Load Vector

Solving Equations

Convergence?

N

Update parameters of interface element and Inherent strains according to assembly stages

Y

Displacement, Stress, Gap, Misalignment

Are all joints welded?

N

Y

End

Fig. 5 Computational approach of elastic FEM

insignificant value. Because the out-of-plane deformations are very small in the cross-shaped joint, only the in-plane inherent deformations (Tendon force and transverse shrinkage) were selected to simulate the overall welding distortion of the large model. The approach to transfer the inherent deformations into inherent strains can be found in Ref. [13, 16].

4.3 Simulation cases

In the current study, four simulation cases were conducted. The detailed information of each case is summarized in **Table 4.** In this study, Case A and Case A' are used to distinguish the simulation results computed by large deformation theory and small deformation theory. Through comparing Case A and Case B, the influence of welding procedure (double-sided welding/single-sided welding) on the final distortion will be clarified. Case B and Case C are used to examine the influence of assembly sequence on the final distortion.

In Case A, Case A' and Case B, it was assumed that all welding lines were welded at the same time. In these three cases, the parameters of interface elements have large values and the stiffness of interface elements is very strong. In Case C, it was assumed that the large structure was assembled by four steps. At the first step, the three longitudinal stiffeners and the skin plate were welded simultaneously. At the second step, the gaps between the transverse stiffeners and the skin plate were corrected through adjusting the parameters of interface elements.

At the third step, four transverse stiffeners and the skin plate were joined simultaneously. At the final step, all cross-shaped joints between the longitudinal stiffeners and the transverse stiffeners were welded at the same time.

5. Simulation results and discussions

5.1 Comparison between large deformation theory and small deformation theory

Fig. 7 compares the deflection distributions along line 1 between Case A and Case A'. It is clear that the deflections calculated by large deformation theory (Case A) are significantly larger than those computed by small deformation theory （Case A'）. From **Fig. 7**, it can be seen that the deflection distribution of Case A' has a symmetric shape. However, the shape of deflection distribution of Case A is significantly asymmetric especially near the two ends. This information suggests that buckling distortion occurred in Case A. **Fig. 8** shows the longitudinal shrinkage distributions of skin plate predicted by Case A and Case A'. The magnitudes of longitudinal shrinkage are the differences between the x-displacements along line 2 and those along line 3. The distribution shape of longitudinal shrinkage predicted by Case A is similar to that calculated by Case A', but the magnitudes of the former are larger than that of the latter. **Fig. 8** also shows that the maximum shrinkage happened at the locations with longitudinal stiffener because these locations are weld zones.

Table 3 Inherent deformations in fillet joint and cross-shaped joint)

Joint	Tendon force (kN)	Trans. shrinkage (mm)	Angular distortion (rad)
Fillet joint (Double-sided welding）	182	0.36	$\beta_1=\beta_2=0.011$
Fillet joint (Single-sided Welding)	116	0.35	$\beta_1\approx\beta_2=0.019$
Cross-shaped Joint	107	0.15 (Long.) 0.14 (Trans.)	Neglected

Table 4 Simulation Cases

Case	Detailed information
Case A	Simultaneous welding; double-sided welding procedure (fillet joint); large deformation theory
Case A'	Simultaneous welding; double-sided welding procedure(fillet joint); small deformation theory
Case B	Simultaneous welding; single-sided welding procedure (fillet joint) large deformation theory
Case C	Sequential welding; single-sided welding procedure (fillet joint); large deformation theory

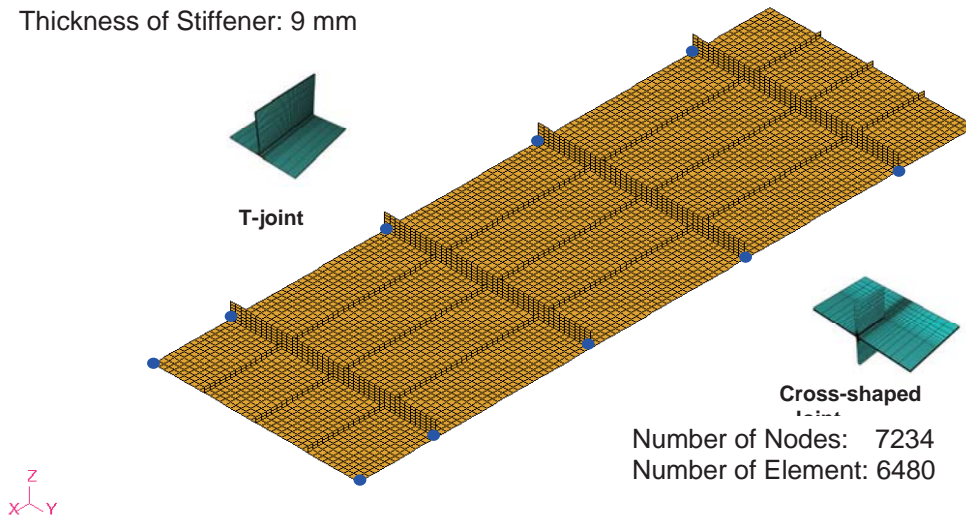Thickness of Skin Plate: 5 mm
Thickness of Stiffener: 9 mm

T-joint

Cross-shaped
Joint

Number of Nodes: 7234
Number of Element: 6480

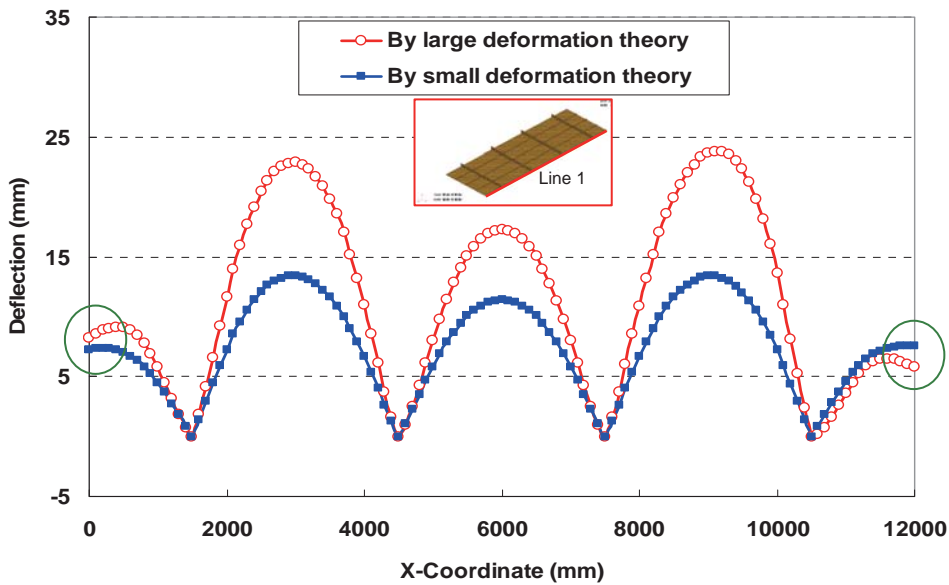**Fig. 6** Finite element model, typical joints and restraint conditions

Fig. 7 Comparison of deflection along line 1 between case A and case A'

Through comparing Case A and Case A', we can conclude that the geometrical nonlinearity should be considered when we predict welding distortion in thin-plate large structures. In such cases, if small deformation theory is used, it will significantly underestimate the welding distortion.

5.2 Influence of welding procedure on final distortion

Fig. 9 shows the contours of deflection distribution predicted by Case A and Case B. The fillet joints in Case A were performed by double-sided welding procedure, while the corresponding joints in Case B were joined by single-sided welding procedure. **Table 3** shows that even

though the total heat input used in the fillet joint is not changed, however the different welding procedure can result in different inherent deformations. For the present fillet joint, double-sided welding procedure produced a larger Tendon force and a smaller angular distortion. Because of different inherent deformation, the final deflection distribution of Case A is significantly different from that of Case B both in magnitude and in shape as shown in **Fig. 9**.

Fig. 10 shows the deflection distributions along line 1. Within the ranges near two ends, not only the magnitudes of deflection predicted by Case B are significantly larger than those simulated by Case A, but also the deflection
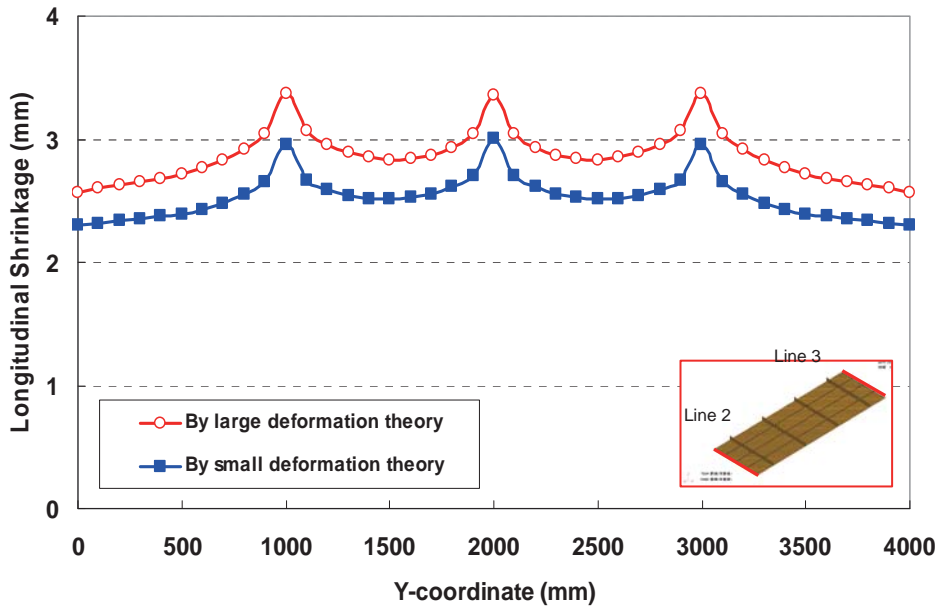
Fig. 8 Comparison of longitudinal shrinkage between case A and case A'
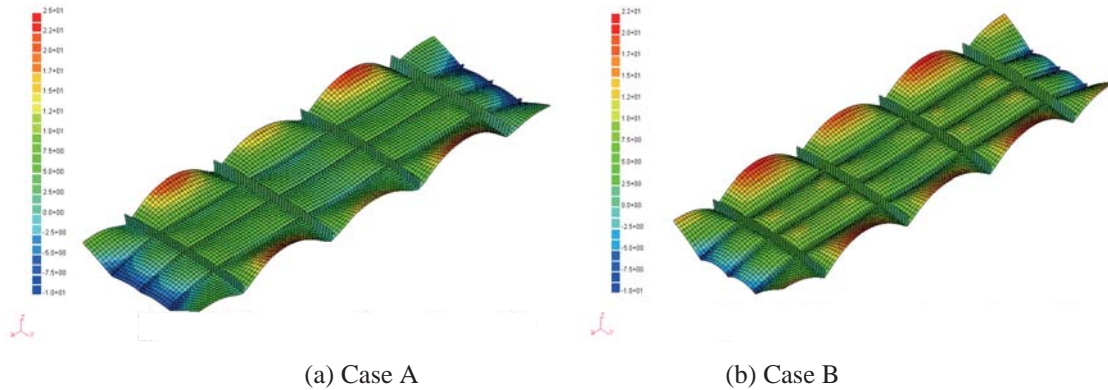

(a) Case A   (b) Case B

Fig. 9 Deflection distributions after welding

distributions shapes of the two cases are different. Here, we pay an attention to the deflection distributions within the range from x=0 mm to x=1500 mm. **Fig. 10** shows that the deflections monotonously decrease within this range in Case B, while the deflection increase within the range from x=0 mm to 400 mm and then decrease in Case A. From **Fig. 10**, we can also see that the magnitudes of deflection near the left end are larger than those near the right ends. This information clearly indicates that buckling distortion occurred in Case A. The larger tendon force induced by double-sided welding producer is the reason resulting in buckling distortion in Case A.

Within the range between x=1500 mm and x=4500 mm, we can see that the deflections of Case A are almost the same as those of Case B, but only the maximum value is a bit larger than that of Case B. Within the range between x=7500 mm and x=10500 mm, we can see that the deflections of Case A are slightly larger than those of Case B on the whole, and the peak value of Case A is clearly

larger than that of Case B. Although the angular distortion of fillet joint in Case A is smaller that in Case B, Tendon force is significantly larger than that in Case B. In principle, Tendon force (or longitudinal shrinkage) is the most important factor resulting in longitudinal bending and buckling distortion. In a welded structure, the total out-of-plane deformation is commonly determined by the longitudinal bending resulting from Tendon force and the deflection caused by angular distortion. Based on the above discussion, it is not difficult to understand that even though the inherent deformations in these two cases are markedly different, the final deflections within the above two ranges have no significant difference.

Within the range between x=4500 mm and x=7500 mm, the deflections of Case A are lower than those of Case B. The local restraint intensity of this range is larger than that of the other range, so the longitudinal bending caused by Tendon fore is restrained to some extent. In such situation, angular distortion seems to make a larger
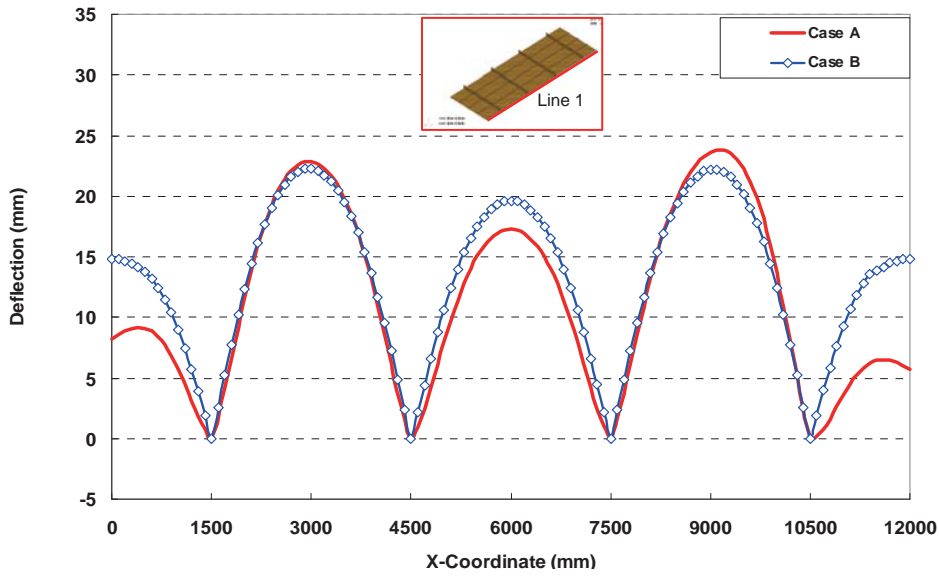
Fig. 10 Deflection distributions along line 1 predicted by Case A and Case B

(a) After the first welding

(b) After correcting gaps

(c) After the second welding
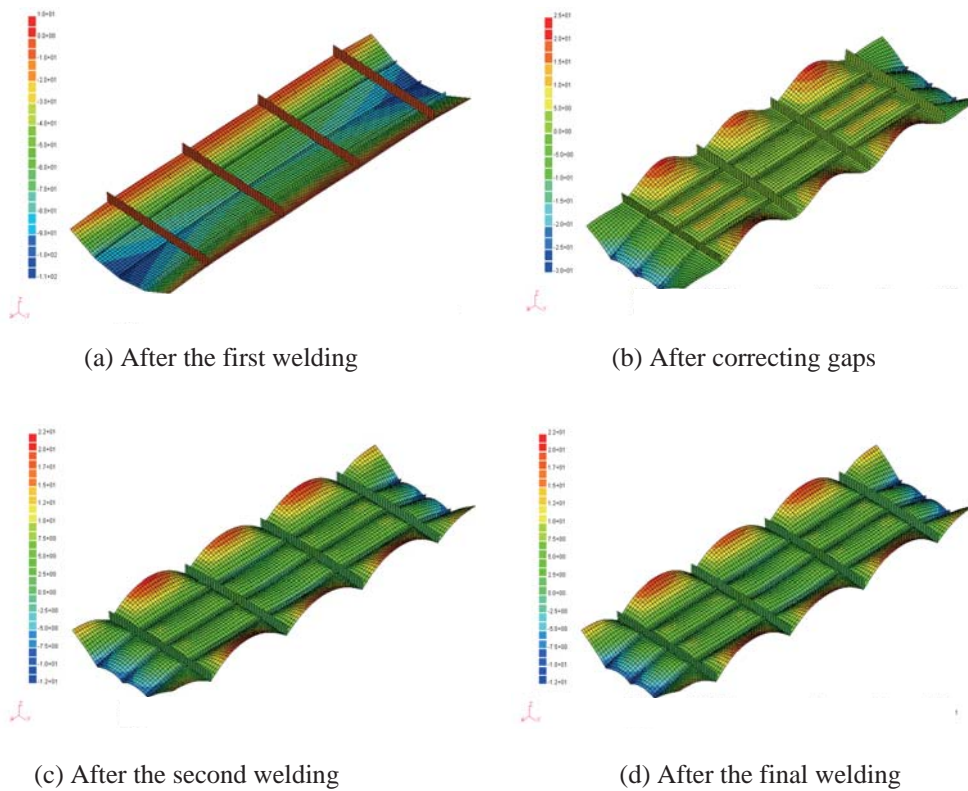

(d) After the final welding

Fig. 11 Deflection distribution changes during assembly process

contribution to the magnitude of deflection.

Comparing Case A and Case B，we can also find that the deflection distribution along line 1 predicted by Case B has symmetrical shape, but that predicted by Case A is asymmetric. The simulation results suggest that welding procedure has a significant influence on the final welding deformation.

5.3 Influence of assembly sequence on final distortion

In this section, we will discuss the influence of assembly sequence on the final distortion. Firstly，we examine the welding deformations produced during assembly process in Case C. **Fig. 11** shows the contours of deflection distributions after all assembly steps in Case C. It is clear that very large deflections are produced after the
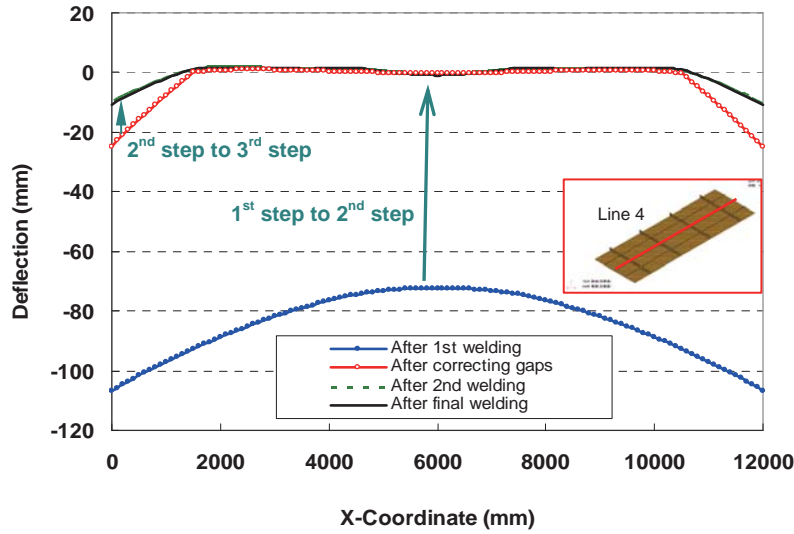
Fig. 12 Deflection distributions along line 4 after each assembly step

first welding because of the relatively small stiffness and the large angular distortion. From **Fig. 11 (a)**, we can see that there are large gaps between the transverse stiffeners and the skin plate, and we can also infer that the maximum gap is over 80 mm. In such situation, if the gaps are not corrected it will be impossible to perform the remaining welding lines. After correcting the gaps, the deflection distribution sharply changed as shown in **Fig. 11 (b)**. Comparing **Fig. 11(a)** and **Fig. 11 (b)**, we can find that gap correction can largely reduce the magnitude of welding deformation. After welding the transverse stiffeners and the skin plate, the deflection distribution changed to some extent both in magnitude and in distribution shape as shown in **Fig. 11 (c)**. **Fig. 11 (d)** shows the deflection distribution after the final welding. The final welding

seems to have no significant contribution to the total deflection, so we can see that the difference between **Fig. 11 (c)** and **Fig. 11 (d)** is very small.

The deflection distributions along line 4 after each assembly step are plotted in **Fig. 12.** Line 4 is the centerline of the skin plate, and it is located at the place of the middle longitudinal stiffener. This figure clearly shows the changes of deflection distribution during the entire assembly process. The change tendency is similar to that reflected in **Fig. 10**.

Through comparing Case B and Case C, we can examine the influence of assembly sequence on the final distortion. The deflection distributions along line 2 and line 4 are plotted in **Fig. 13** and **Fig. 14**, respectively. The
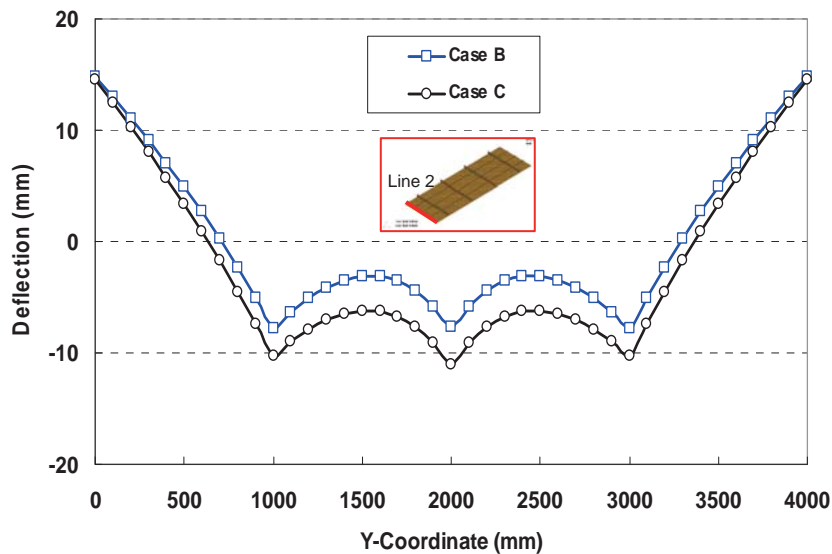

Fig. 13 Deflection distribution along line 2 predicted by Case B and Case C

deflection distributions along the two compared lines predicted by the two cases have similar shape, but the magnitudes of welding distortion in Case C are large than those in Case B on the whole. Because all parts were welded at the same time in Case B, the stiffness was a constant during welding and its value was relatively large. In addition, there was not any gap between parts in this case. On the contrary, the stiffness in Case C changed (increased) with assembly proceeding, and it was relatively small at the first assembly step. Moreover, large gaps between the transverse stiffeners and the skin plate generated after the first welding. Even though the gaps were corrected to a certain extent at the second step, but they were not completely closed. Considering the above factors, it is easy to understand that the magnitude of welding deformation in Case C is larger than that in Case B.

The comparison between Case B and Case C indicates that the assembly sequence has a relatively large influence on the final welding distortion.

6. Conclusions

The welding distortion in a large thin-plate panel structure was predicted by means of elastic FEM based on inherent strain theory and interface element formulation. The influence of welding procedure on the final distortion was clarified numerically. In addition, the influence of assembly sequence on the final welding distortion was investigated. Based on the simulation results, the following conclusions can be drawn.

Because the stiffness of a thin-plate welded structure is relatively small, geometrical nonlinearity is apt to occur during assembly process. When the elastic FEM is used to predict welding deformation in a thin-plate structure, the large deformation theory should be involved in the elastic FEM.

1) Simulation results suggest that welding procedure has a certain influence on the final welding distortion. Double-sided welding procedure can produce a larger tendon force, so it can increase the buckling propensity especially in thin-plate structures.

2) Based on the simulation results, we have known that the assembly sequence has a significant influence on the final distortion. The present work suggests that sequential welding will increase welding distortion.

3) The proposed elastic FEM not only may be used to estimate welding deformation of a large and complex structure in the design stage, but also can be employed to optimize welding procedure during the manufacturing stage.

References

1) M. Watanabe, K. Satoh, Fundamental study on buckling of thin steel plate due to bead-welding, Journal of the Japan Welding Society, 27(6), 1958, pp.313-320.

2) T. Nomoto, T. Terasaki, K. Maeda, Study of parameters controlling weld buckling, Transaction of the Japan Society of Mechanical Engineering, Series A, 63(609), 1997, pp.591-596.

3) T. Terasaki, K. Maeda, H. Murakawa, T. Nomoto, Critical conditions of plate buckling generated by welding, Transaction of the Japan Society of Mechanical Engineers A, 64(625), 1998, pp.2239-2244.

4) C. L. Tsai, M. S. Han, G. H. Jung, Investigating the bifurcation phenomenon in plate welding, Welding Journal, 2006, pp.151s-162s.

5) S. R. Bhide, P. Michaleris, M. Posada. J. Deloach, Comparison of buckling distortion propensity for SAW, GMAW, and FSW welding, Welding Journal, 2006, pp.189s-195s.

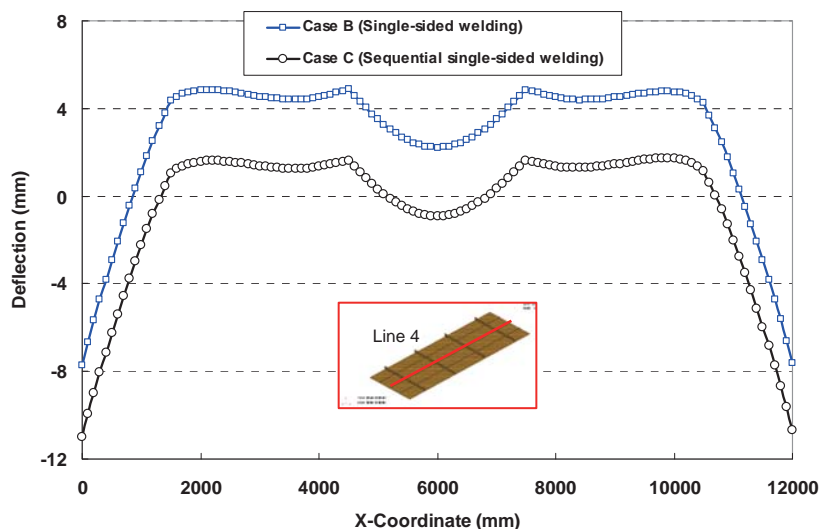6) T. D. Huang, P. Dong, L. A. DeCan, D. D. Harwig, Residual stress and distortion in lightweight ship panel

Fig. 14 Deflection distribution along line 4 predicted by Case B and Case C

structures, Technology Review Journal (Spring/Summer), 2003, pp.1-26.

7) T. D. Huang, P. Dong, L.A. DeCan, D. D. Harwig, R. Kumar, Fabrication and engineering technology for lightweight ship structures, Part 1: Distortion and residual stresses in panel fabrication, Journal of Ship Production, 20(1), 2004, pp.43-49.

8) M. V. Deo, P. Michaleris, Mitigation of welding induced buckling distortion using transient thermal tensioning, Science and Technology of Welding and Joining, 8(1), 2003 , pp. 49-54.

9) P. Michaleris, Modelling welding residual stress and distortion: current and future research trends, Science and Technology of Welding and Joining, 2011, 16(4), pp.363-368.

10) H. Murakawa, D. Deng, S. Rashed, S. Sato, Prediction of distortion produced on welded structures during assembly using inherent deformations and interface element, Transactions of JWRI, Vol. 38(2), 2009, pp.63-69.

11) J.D. White, R.H. Leggatt, J. B. Dwight, Weld shrinkage prediction, Welding Metal Fabrication,1980, pp.567-596.

12) G. Verhaeghe, Predictive Formulate for Weld

Distortion-A Critical Review, Abingto Publishing, 2000.

13) D. Deng, H. Murakawa, W. Liang, Numerical simulation of welding distortion in large structures, Computer methods in applied mechanics and engineering, 196, 2007, pp.4613-4627.

14) S. P. Timoshenko, S. Woinowsky-Krieger, Theory of Plates and Shells, McGraw-Hill Book Company, 1959.

15) H. Murakawa, D. Deng, M. Shibahara, Prediction of welding distortion during the assembly process of thin plate structures, Journal of the Kansai Society of Naval Architects, 238, 2002, pp.163-172.

16) D. Deng, H. Murakawa, W. Liang, Prediction of welding distortion in a curved plate structure by means of elastic finite element method, Journal of Materials Processing Technology, 203, 2008, pp.252-266.

17) Robert W. Messler, Jr., Principles of Welding, Process, Physics, Chemistry and Metallyury, A Wiley-Interscience Publication, 1999.

18) D. Deng, W. Liang, H. Murakawa, Determination of welding deformation in fillet-welded joint by means of numerical simulation and comparison with experimental measurements, Journal of Materials Processing Technology, 198, 2007.